CHINESE OPTICS LETTERS

Vol. 22, No. 8 | August 2024

Toward a compact fiber comb with 1.66×10^{-12} instability based on acetylene-filled photonic microcells

Qingqing Chen (陈清清), Yongqi Li (李勇琪), and Shun Wu (吴 舜)*

Hubei Key Laboratory of Optical Information and Pattern Recognition, Wuhan Institute of Technology, Wuhan 430205, China

*Corresponding author: wushun_wit@163.com

Received January 4, 2024 | Accepted April 10, 2024 | Posted Online August 13, 2024

We demonstrated an optical fiber frequency comb stabilized to an acetylene-filled photonic microcell. The short-term instability of the comb at 1 s gate time was 1.66×10^{-12} for a 4.2-h measurement in a laboratory environment with air conditioning. This is the best short-term stability reported for a compact fiber comb stabilized to an acetylene-filled photonic microcell at telecom wavelengths. It is particularly significant in the development of compact fiber combs with target instability of 10^{-13}. Such a device has the potential to serve as an alternative to GPS in areas lacking signal coverage, including remote locations, regions with adverse weather conditions, and military intelligence areas.

Keywords: optical frequency comb; gas-filled photonic microcell; hollow-core photonic crystal fiber.
DOI: 10.3788/COL202422.080601

1. Introduction

In the past decade, research on optical fiber frequency combs (OFCs) has led to an increasing demand for outdoor combs that offer both high stability and portability[1–9]. The instability of an OFC relies on the phase stabilization of carrier envelope offset frequency (f_{ceo}) and repetition rate (f_r). It is common to stabilize both parameters to an RF reference[10–15]. However, the uncertainty of the RF reference can be magnified for optical frequencies. To improve comb's fractional stability, either a fiber comb with high repetition rate (GHz) or an RF reference with better performance, such as a "hydrogen" maser and "cesium" clock, is utilized. The bulk nature of these RF references makes them less desirable for portable fiber comb systems. Stabilization of f_{ceo} can be achieved through the $f-2f$ self-reference method, but it requires a broadened spectrum and high optical power, which in turn leads to increased system complexity and sensitivity to the environment.

Another stabilization method is to lock the comb to optical references, such as an optical cavity or an atomic or molecular reference[13,16–22]. Ultrastable Fabry–Perot (F–P) cavities have excellent short-term instability, but require vacuum and vibration isolation, which are difficult to satisfy in field applications[23–28]. In comparison, gas absorption transitions can offer excellent long-term instability and absolute frequency accuracy[29–31]. They are also cost-effective and convenient to miniaturize[32]. By stabilizing a single comb mode to an atomic or molecular reference, the instability of the optical reference can be transferred to the comb. In 2014, Hou *et al.* demonstrated an erbium fiber comb referenced to two rubidium absorption lines through frequency doubling and two-photon absorption technique. The comb mode shows a short-term instability of 8×10^{-11} at 1 s gate time[33]. A disadvantage of the system to outdoor applications is that the sensitivity of rubidium pressure changes with temperature. In 2014, Wu *et al.* directly amplified a single comb mode and locked it to an acetylene transition[34]. The comb demonstrated an instability of 6×10^{-12}. However, the system involved a free-space F–P cavity that was bulky and complex.

Instead of directly stabilizing a comb mode to an optical reference, a simpler option is to stabilize the optical heterodyne beat note between a continuous wave (cw) reference and a comb mode[35–40]. A technical challenge in using molecular transitions as optical references is their limited instability, due to the broad linewidth of over gigahertz. Saturated absorption spectroscopy (SAS) can significantly reduce the Doppler broadening and can achieve linewidths of tens of megahertz at room temperature by velocity-selective optical pumping. By utilizing a low-pressure gas-filled hollow-core photonic crystal fiber (PCF) as a substitute for the Herriott cell, we can effortlessly enhance the interaction strength by using long length of hollow-core fiber, and meanwhile, reduce the pressure-broadening effect. A photonic microcell can serve as a potential portable cw reference for outdoor metrology applications[41–43]. Hald *et al.* from the Danish Metrology Institute achieved slow-molecule conditions and realized the Doppler-free linewidth exceeding the limit imposed by the transit-time broadening[44]. They demonstrated an optical cw reference with long-term instability of 4×10^{-12} at 10,000 s gate time[45]. In 2017, they stabilized the commercial fiber comb from MenloSystems to a 50 cm double-pass acetylene

cell and obtained a fractional instability of 3×10^{-13} at 1 s gate time[31,46].

In this paper, we explored the fractional instability performance of a homemade optical fiber frequency comb stabilized to an acetylene-filled photonic microcell. Compared to Ref. [31], our comb system is more compact and portable. The microcell in this work was a 2.1 m 19-cell hollow-core PCF. We optimized the characteristics of the sub-Doppler absorption feature for two absorption lines: the P (13) and P (23) lines of the $^{12}C_2H_2$ $\nu_1 + \nu_3$ overtone transition. By stabilizing the repetition rate and the RF beat note, the high stability of the optical reference is transmitted to other wavelengths through the comb. The comb shows a repetition rate instability of 4.87×10^{-12} at 1 s gate time and 2.79×10^{-13} at 100 s gate time, with a standard deviation (SD) of 0.4 mHz. The short-term instability of the beat note at 1 s gate time is 1.66×10^{-12} for a measurement of 4.2 h. This work represents the highest short-term instability for a compact optical fiber frequency comb stabilized to an optical reference of acetylene-filled photonic microcell.

2. Experimental Setup

Figure 1 shows the schematic diagram of optical fiber frequency comb stabilization based on the acetylene-filled microcell. The upper dashed box shows the frequency stabilization of a narrow linewidth cw laser to the sub-Doppler absorption feature of acetylene. The gas cell was a 19-cell hollow-core PCF with a core diameter of 30 μm and length of 2.1 m filled with low-pressure acetylene. The sub-Doppler absorption feature was produced using the pump–probe scheme[47]. A cw laser was optically amplified before it was split into two counter-propagating pump and probe beams and interacted with the acetylene molecules in the gas cell. The probe beam exiting the PCF was separated from the pump by a polarization beam splitter (PBS) and received by the photodetector (New Focus, Model 1623). The sub-Doppler resonance was frequency-shifted by a 55 MHz acousto-optic modulator (AOM) to reduce noise due to pump–probe interference. By employing frequency modulation (FM) spectroscopy[25,48], an error signal was generated to stabilize the probe beam to the sub-Doppler feature. An in-line polarizer was used in the probe line to minimize the residual amplitude modulation (RAM). The output of the proportional-integral-differential (PID) circuit was fed to the cw laser's piezo-electric transducer (PZT) for precise frequency control. Thus, the stabilized cw laser can serve as an optical reference for the fiber comb. The lower dashed box illustrates the stabilization system of a fiber comb referenced to the cw reference. The all-fiber erbium laser oscillator was mode-locked based on nonlinear polarization rotation (NPR). The laser was first filtered by a fiber Bragg grating (FBG) centered at 1532.83 nm and then optically heterodyne beaten against the cw reference, resulting in an RF beat note f_b. The stabilization of the comb was achieved by simultaneously locking the f_b and repetition rate f_r to two separate synthesizers referenced to the Rb oscillator. Our tests showed that the PZT electronic bandwidth was 3 kHz under 1.25% amplitude modulation, while the locking bandwidth for the pump diode was measured to be 22 kHz.

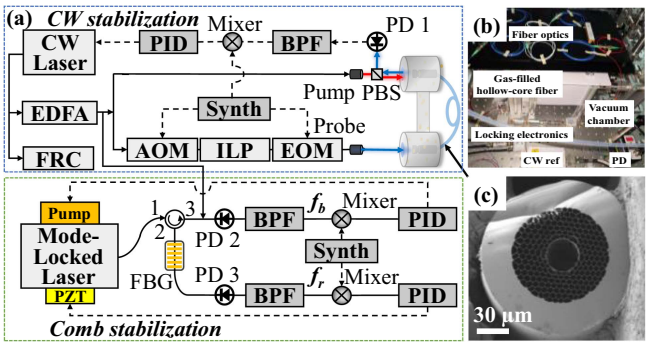

Fig. 1. (a) Schematic diagram of optical fiber frequency comb based on acetylene saturated absorption spectroscopy frequency stabilized optical reference. The black solid line represents the optical signal, the fluorescent solid line represents the free-space optical signal, and the black dashed line represents the RF signal. cw laser, continuous-wave laser; FRC, fiber-ring cavity; EDFA, erbium-doped fiber amplifier; AOM, acousto-optic modulator; ILP, in-line polarizer; EOM, electro-optic modulator; PBS, polarization beam splitter; PD, photodetector; Synth, synthesizer; BPF, bandpass filter; PID, proportional-integral-differential circuit; FBG, fiber Bragg grating; PZT, piezoelectric transducer; HC-PCF, hollow-core PCF. (b) Photo of the actual setup; (c) SEM image of the cross section of the hollow-core fiber.

3. Results and Discussion

3.1. Acetylene SAS-stabilized semiconductor laser

A narrow linewidth of the sub-Doppler feature is essential for frequency stabilization of the cw reference. In this section, we discuss the optimization of the sub-Doppler absorption feature in a gas-filled photonic microcell for two separate transition lines: P (13) and P (23) lines of $^{12}C_2H_2$ $\nu_1 + \nu_3$ overtone transition.

Figures 2(a) and 2(b) show the measured sub-Doppler absorption feature (black) for P(13) and P(23) line, respectively. The blue curve was the resonance peaks from a fiber-ring cavity (FRC) as the cw laser frequency was scanned, serving as the calibration reference for the sub-Doppler linewidth. Any two adjacent transmission peaks represented the free spectral range (FSR) of the FRC, which was measured to be 17.1 ± 0.1 MHz. As shown in Fig. 2(b), the SNR of sub-Doppler feature was determined as the ratio between the peak-to-peak voltage of the feature (A) and that of the background noise (B). We measured the linewidth and SNR at various acetylene pressures and pump powers, represented by black squares and blue hollow triangles in Figs. 2(c)–2(f). We observed that for the P(13) line, under a constant pump power of 29 mW, the linewidth of the sub-Doppler feature remained around 15 MHz in the pressure range of 150–1000 mTorr, followed by an small increase at higher pressures due to collision broadening. The SNR showed a nonmonotonic behavior with the pressure. Figure 2(d) further

investigates how the pump power influences the sub-Doppler feature. The linewidth was about 15 MHz before the pump power increased to a threshold saturation power of 35 mW when the linewidth started to exhibit evident power broadening. Under a threshold pressure, the increase in pump power can still keep the acetylene molecules under a saturation condition, thereby enhancing the SNR of the sub-Doppler feature. The optimized acetylene pressure was 600–700 mTorr when a highest SNR of ~42 and ~15.1 ± 1.3 MHz linewidth were obtained for the P (13) line. We estimated the transit-time broadening under this condition at room temperature. Considering the mode field diameter (MFD) of the PCF was 20 μm, the transit-time broadening was estimated to be ~16.3 MHz, which was consistent with our experimental result.

Compared to the P (13) line, the P (23) line showed a weaker absorption of ~10% rather than ~40% for that of the P (13) line. In Figs. 2(e) and 2(f), a similar trend for linewidth was observed. As for the SNR, since the P (23) line has weaker absorption strength, when the pressure increased above 550 mTorr, the pump power of 29 mW (or more) could still satisfy the saturation condition and therefore a similar SNR was obtained. Due to the stronger power broadening and a lower saturated pump threshold, we obtained a lower SNR and a larger linewidth for the P (23) line than that of the P (13) line under the same

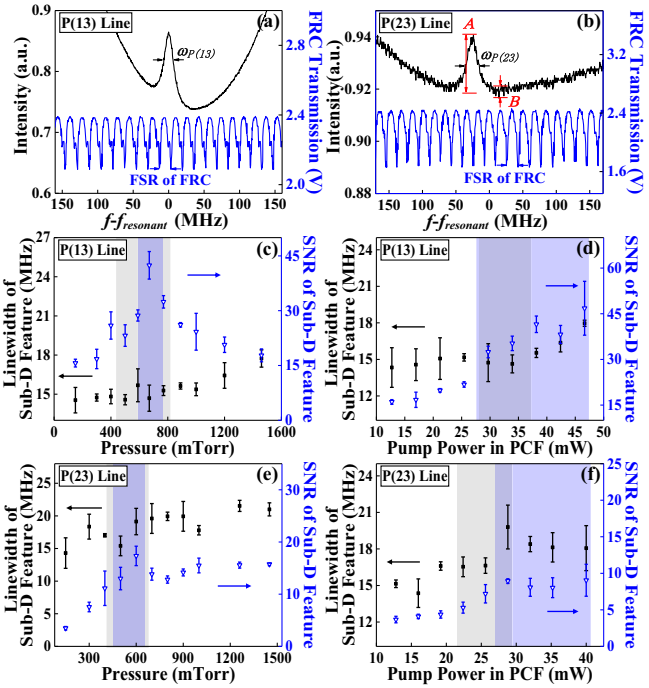

Fig. 2. Optimized condition for a 2.1-m-long acetylene-filled microcell: (a) normalized sub-Doppler absorption spectrum for the P (13) line (left axis) and transmission spectrum for a fiber ring cavity with FSR of 17.1 ± 0.1 MHz (right axis); (b) same as (a) for the P (23) line; linewidth and SNR for the sub-Doppler feature of the P (13) line as a function of (c) acetylene pressure (under pump power of 29 mW) and (d) pump power (at pressure of 650 mTorr); (e) same as (c) for the P (23) line; (f) same as (d) for the P (23) line (at 600 mTorr).

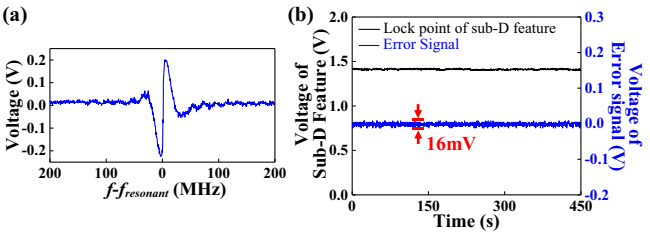

Fig. 3. (a) Frequency modulation spectroscopy error signal of the P (13) transition; (b) lock point voltage and error signal of P (13) transition after being locked. The amplitude of error signal was less than 16 mV.

pressure and power conditions. In summary, when the acetylene pressure was in the range of 550–650 mTorr and the pump optical power was ~29 mW, the optimized sub-Doppler absorption feature of the P (23) line in the 2.1-m microcell had the narrowest linewidth of ~18.4 ± 1.2 MHz with an SNR of ~18.

Considering the sub-Doppler characteristics and the error signal parameters generated from frequency modulation spectrum, the P (13) line was finally chosen as the optical reference for the cw reference. Figure 3(a) shows the error signal produced, with a slope of 19.3 kHz/mV and an SNR of 43. When the cw laser was stabilized to the sub-Doppler transition, the error signal became flat, as shown in Fig. 3(b). Another proof was that when the laser was locked, the transmission remained at the peak of the sub-Doppler absorption feature.

3.2. Stabilization of OFC based on optical reference

In this section, we stabilize an all-fiber comb to the cw reference, and analyze the fractional instability of the comb. Figure 4(a) shows the optical spectrum of the fiber oscillator measured by an optical spectrum analyzer (OSA, Yokogawa, AQ6370C) at a resolution of 0.02 nm. The fiber oscillator we used was a typical soliton mode-locked laser with symmetrical Kelly sidebands based on NPR. The central wavelength of the mode-locked spectrum was shifted to 1534 nm by introducing a Lyot filtering element in the laser cavity[49]. The comb was stabilized by simultaneously locking (i) the repetition rate frequency f_r and (ii) the optical heterodyne beat note f_b between the comb and the cw reference. Figure 4(b) presents the RF spectrum of a 97.36 MHz repetition rate with an SNR of 65 dB and a pair of optical heterodyne beat notes with an SNR of 32 dB at 100 kHz resolution bandwidth (RBW).

For repetition rate stabilization, our results in Fig. 4(c) exhibited an SD of 0.4 mHz after locking f_r to a frequency synthesizer referenced to the Rb oscillator. The data showed small periodic variations that were consistent with the duty cycle of the air conditioner in the lab. For beat note f_b stabilization, we first filtered the comb modes by an FBG centered at 1532.83 nm, and then performed an optical heterodyne beat against the cw reference laser. The resulting RF beat note was stabilized to a frequency synthesizer by pump power control. All synthesizers and frequency counters were referenced to the Rb oscillator. Figure 4(d) shows the raw data of the stabilized beat note signal measured

in 4.2 h, indicating a maximum frequency fluctuation of about 20 kHz. The periodic oscillations were correlated with temperature fluctuations in the lab. The inset in Fig. 4(d) presents the processed beat note result after we removed the temperature oscillations from the raw data, indicating that with proper temperature control of the fiber oscillator, it is possible to expect that the fluctuation of f_b can be reduced to about 3 kHz.

Figure 5(a) illustrates the postprocessed beat note data after we filtered the low-frequency components introduced by the environmental vibrations or temperature fluctuations. We evaluated the locking performance of the comb by calculating the fractional instability of f_r and f_b and compared that with our RF reference signal, as plotted in Fig. 5(b). The green down-triangles and blue up-triangles represent the instability of the Rb oscillator and synthesizers referenced to the Rb oscillator, respectively. The fractional instability of f_r, plotted in black squares, followed the synthesizer performance, as expected, and was measured to be 4.87×10^{-12} at 1 s gate time and 2.79×10^{-13} at 100 s gate time.

Since the optical frequency of the cw reference is stabilized to the absorption line of acetylene, using a combs equation, we can derive the absolute frequency for the comb mode of interest, i.e., the mth mode: $f_m = (f_{cw} - f_b) + (m - n) \times f_r$. f_{cw} is the absolute frequency of the cw reference, and n is the mode number for the particular comb mode that is stabilized to the cw reference. f_b and f_r are the beat note and repetition frequency, respectively. When m is close enough to n, the second term can be neglected compared to the first. Therefore, the absolute frequency of the mth comb mode is largely determined by the absorption line of acetylene. This is exactly what we have observed in Fig. 5(b), where the fractional instability of f_b was 1.66×10^{-12} at 1 s gate time, indicated by the red circle, surpassed the performance of the repetition rate at a short time scale. This indicated that the stability of the cw reference was successfully transmitted to that of the comb mode.

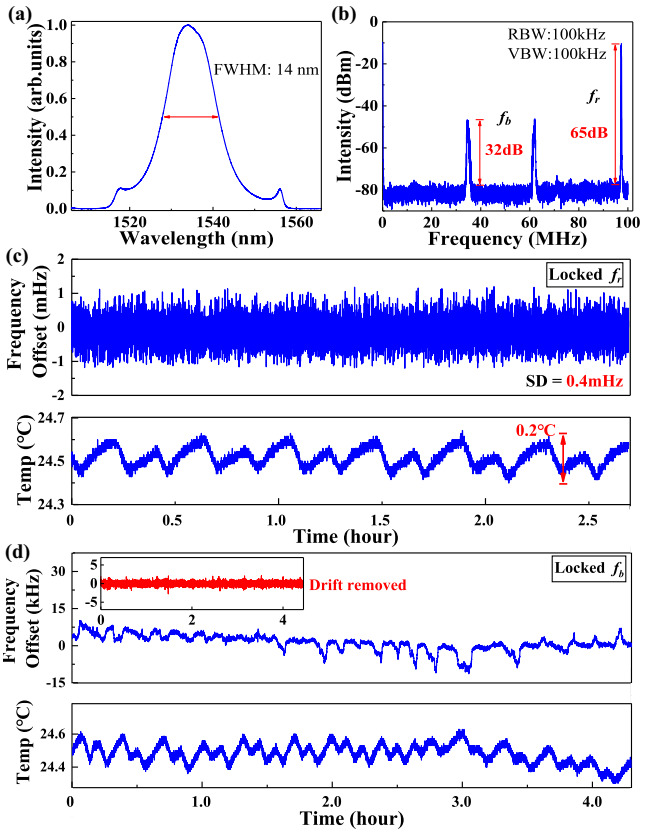

Fig. 4. (a) Optical spectrum of the fiber oscillator in linear scale; (b) RF spectrum of the repetition rate and the heterodyne beat note (RBW, 100 kHz; VBW, video bandwidth); (c) stabilized repetition frequency measured at 1 s gate time with SD of 0.4 mHz (data subtracted by ~97.36 MHz); (d) stabilized beat note frequency measured at 1 s gate time. Inset shows the processed data after the periodic oscillations due to temperature fluctuations were removed.

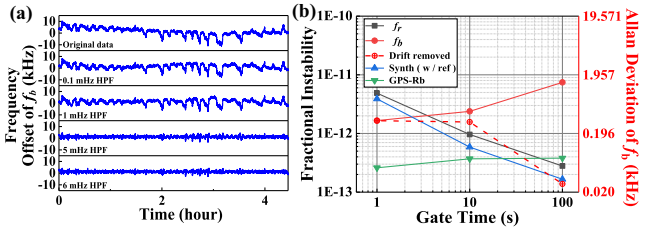

Fig. 5. (a) Postprocessed beat note data after we added high-pass filters (HPFs); (b) fractional instability (left) and Allan deviation (right) of the RF beat note f_b between the comb and the cw reference at 1532.8 nm (red dots) compared to that of the repetition rate (black squares), data in (a) with 5 mHz HPF (red cross circle), synthesizer signal with external reference (blue up-triangles), and GPS-disciplined Rb oscillator (green down-triangles).

However, as shown in Fig. 5(b), the fractional instability of f_b deteriorated at longer gate times (i.e., 2.38×10^{-12} and 7.43×10^{-12}, for 10 s and 100 s gate time, respectively). This was due to the fluctuations of the ambient temperature in the lab. This could be improved by implementing active temperature control or heat insulation. To qualitatively estimate the long-term instability of our comb, we performed post-data processing by removing the duty cycle oscillations in the raw beat note data due to periodic temperature variations. For example, by using a 5 mHz high-pass filter (HPF) as shown in Fig. 5(a), we obtained the red cross circles in Fig. 5(b). The results suggested that a fractional instability on the order of 10^{-13} could possibly be achieved at longer time scales. This corresponds to an ambient temperature fluctuation of less than 0.13°C according to our estimation.

Generally speaking, the fractional stability of the optical heterodyne beat note is affected by the linewidth, the SNR of the RF beat, and the electronic locking loop for beat note stabilization. In our system, there are mainly two consequences from temperature fluctuation. On one hand, it causes the spectral variation of the mode-locked oscillator. Although we did not observe any obvious spectral shift or optical power change on the spectrum analyzer, consider that the optical power for a single comb mode at 1532.83 nm is on the order of tens of nanowatts, and so any slight variation in the mode-locked spectrum will affect the beat note. On the other hand, the RAM from EOM

in the cw stabilization system led to small temporal variation of the error signal for cw reference stabilization. Since the EDFA and hollow-core fiber we used were both non-PM, an inline polarizer was intentionally added to reduce the RAM effect. However, the RAM effect was not entirely eliminated. The overall SNR change of the beat note we observed during the measurement is less than 2 dB. The long-term instability of the beat note is mostly due to the small voltage offset in the beat note electronic feedback loop, which causes the slow drift of the lock point. This can be improved by removing the offsets in the locking electronics.

4. Conclusions

We experimentally demonstrated a fiber laser frequency comb with 1.66×10^{-12} instability based on a low-pressure acetylene-filled photonic microcell. By performing a pump–probe scheme inside a $^{12}C_2H_2$-filled hollow-core PCF, we were able to obtain the sub-Doppler absorption feature of both P (13) and P (23) lines of the $\nu_1 + \nu_3$ overtone transition at room temperature. The optimized linewidth of the sub-Doppler feature was about 15.1 MHz with an SNR of 42 for the P (13) line. An optical cw reference was realized by stabilizing a narrow linewidth cw laser to the sub-Doppler feature of the P (13) line at 1532.8 nm through FM spectroscopy. Finally, we demonstrated the stabilization of an optical fiber frequency comb with one comb mode locked to the cw reference. The comb showed the repetition rate instability of 4.87×10^{-12} at 1 s, and 2.79×10^{-13} at 100 s gate time, with an SD of 0.4 mHz. The short-term instability of the heterodyne beat note f_b between the comb and the cw reference at 1 s gate time was 1.66×10^{-12} over a measurement of 4.2 h. This result is the best short-term instability reported for a fiber comb stabilized to a gas cell at telecom wavelengths. With proper temperature control of the fiber oscillator, we anticipate the system instability to reach 10^{-13} at 100 s gate time.

Previously published work includes the traditional f_{ceo} stabilization utilizing the $f-2f$ technique[50,51], and a single comb mode stabilized to an ultrastable F–P cavity[52,53]. For both methods, the fractional instability of f_{ceo} can reach 10^{-17}–10^{-18}. However, the optical frequency instabilities usually were not reported. Compared to the f_{ceo}-stabilized combs, our system does not require excess optical amplification to generate a supercontinuum. Utilizing molecular absorption lines as the optical reference is expected to have better long-term instability than ultrastable F-P cavities, in addition to having better portability. The cw reference based on saturated absorption spectroscopy (SAS) in this work was obtained using a microcell installed with small vacuum chambers. We are currently working on the miniaturization of the acetylene microcell with the SAS setup. The dimensions of the miniaturized microcell are $7\,\mathrm{cm}(W) \times 17\,\mathrm{cm}(L) \times 4.6\,\mathrm{cm}(H)$. It would greatly reduce the volume of the existing system and serve as the high stability cw reference for a portable all-fiber comb system with target instability of 10^{-13}. Our scheme offers much promise as a compact, portable, and inexpensive optical fiber frequency comb with high stability, surpassing that of the GPS-disciplined Rb oscillator. Our system has the potential to serve as a substitute for GPS in areas where signal coverage is lacking (for example, remote locations, regions with adverse weather conditions, and military intelligence areas).

Acknowledgements

This work was supported by the Campus Science Foundation of Wuhan Institute of Technology (No. 22QD01), the Open Research Fund of State Key Laboratory of Transient Optics and Photonics (No. SKLST202105), and the Hubei Province Natural Science Foundation (No. 2023AFB778).

References

1. V. Brasch, E. Lucas, J. D. Jost, *et al.*, "Self-referenced photonic chip soliton Kerr frequency comb," Light Sci. Appl. **6**, e16202 (2016).
2. S. Droste, G. Ycas, B. R. Washburn, *et al.*, "Optical frequency comb generation based on erbium fiber lasers," Nanophotonics **5**, 196 (2016).
3. J. Lim, K. Knabe, K. A. Tillman, *et al.*, "A phase-stabilized carbon nanotube fiber laser frequency comb," Opt. Express **17**, 14115 (2009).
4. T. Fortier and E. Baumann, "20 years of developments in optical frequency comb technology and applications," Commun. Phys. **2**, 153 (2019).
5. W. Xia and X. Chen, "Recent developments in fiber-based optical frequency comb and its applications," Meas. Sci. Technol. **27**, 041001 (2016).
6. X. Cao, J. Zhou, Z. Cheng, *et al.*, "GHz figure-9 Er-doped optical frequency comb based on nested fiber ring resonators," Laser Photonics Rev. **17**, 2300537 (2023).
7. S. M. Schweyer, B. Eder, P. Putzer, *et al.*, "All-in-fiber SESAM based comb oscillator with an intra-cavity electro-optic modulator for coherent high bandwidth stabilization," Opt. Express **26**, 23798 (2018).
8. X. Xu, Z. Zhang, H. Zhang, *et al.*, "Long distance measurement by dynamic optical frequency comb," Opt. Express **28**, 4398 (2020).
9. A. Moreno-Oyervides, O. E. Bonilla-Manrique, O. García, *et al.*, "Design and evaluation of a portable frequency comb-referenced laser heterodyne radiometer," Opt. Lasers Eng. **171**, 107801 (2023).
10. T. Udem, R. Holzwarth, and T. W. Hänsch, "Optical frequency metrology," Nature **416**, 233 (2002).
11. M. J. Thorpe, D. Balslev-Clausen, M. S. Kirchner, *et al.*, "Cavity-enhanced optical frequency comb spectroscopy: application to human breath analysis," Opt. Express **16**, 2387 (2008).
12. D. C. Heinecke, A. Bartels, T. M. Fortier, *et al.*, "Optical frequency stabilization of a 10 GHz Ti:sapphire frequency comb by saturated absorption spectroscopy in ^{87}Rb," Phys. Rev. A **80**, 053806 (2009).
13. A. Benedick, D. Tyurikov, M. Gubin, *et al.*, "Compact, Ti:sapphire-based, methane-stabilized optical molecular frequency comb and clock," Opt. Lett. **34**, 2168 (2009).
14. L. Zhou, X. Qin, Y. Di, *et al.*, "Frequency comb with a spectral range of 0.4–5.2 μm based on a compact all-fiber laser and $LiNbO_3$ waveguide," Opt. Lett. **48**, 4673 (2023).
15. Y. Chang, T. Jiang, Z. Zhang, *et al.*, "All-fiber Yb:fiber frequency comb," Chin. Opt. Lett. **17**, 053201 (2019).
16. Y. Nakajima, H. Inaba, K. Hosaka, *et al.*, "A multi-branch, fiber-based frequency comb with millihertz-level relative linewidths using an intra-cavity electro-optic modulator," Opt. Express **18**, 1667 (2010).
17. R. J. Jones and J.-C. Diels, "Stabilization of femtosecond lasers for optical frequency metrology and direct optical to radio frequency synthesis," Phys. Rev. Lett. **86**, 3288 (2001).
18. E. Fasci, S. Gravina, G. Porzio, *et al.*, "Lamb-dip cavity ring-down spectroscopy of acetylene at 1.4 μm," New J. Phys. **23**, 123023 (2021).
19. J.-R. Chen, T.-H. Suen, C.-Y. Kung, *et al.*, "High stability multiple-frequency cavity locking based on Doppler-free optogalvanic calcium ion spectroscopy," Opt. Express **30**, 28170 (2022).

20. H. Shi, Y. Jiang, Y. Yao, *et al.*, "Optical frequency divider: capable of measuring optical frequency ratio in 22 digits," APL Photonics **8**, 100802 (2023).
21. R. Niu, S. Wan, W. Li, *et al.*, "An integrated wavemeter based on fully-stabilized resonant electro-optic frequency comb," Commun. Phys. **6**, 329 (2023).
22. X. Shao, H. Han, H. Wang, *et al.*, "High power optical frequency comb with 10^{-19} frequency instability," Opt. Express **31**, 32813 (2023).
23. D. Jiao, X. Deng, J. Gao, *et al.*, "Highly vibration-resistant sub-Hertz ultrastable laser passing over 1700 km transport test," Infrared Phys. Technol. **130**, 104608 (2023).
24. E. D. Black, "An introduction to Pound–Drever–Hall laser frequency stabilization," Am. J. Phys. **69**, 79 (2001).
25. G. C. Bjorklund, M. D. Levenson, W. Lenth, *et al.*, "Frequency modulation (FM) spectroscopy," Appl. Phys. B **32**, 145 (1983).
26. L. Jin, "Suppression of residual amplitude modulation of ADP electro-optical modulator in Pound-Drever-Hall laser frequency stabilization," Opt. Laser Technol. **136**, 106758 (2021).
27. M. L. Kelleher, C. A. McLemore, D. Lee, *et al.*, "Compact, portable, thermal-noise-limited optical cavity with low acceleration sensitivity," Opt. Express **31**, 11954 (2023).
28. I. Ito, A. Silva, T. Nakamura, *et al.*, "Stable CW laser based on low thermal expansion ceramic cavity with 49 mHz/s frequency drift," Opt. Express **25**, 26020 (2017).
29. V. Maurice, Z. L. Newman, S. Dickerson, *et al.*, "Miniaturized optical frequency reference for next-generation portable optical clocks," Opt. Express **28**, 24708 (2020).
30. H. Shang, T. Zhang, J. Miao, *et al.*, "Laser with 10^{-13} short-term instability for compact optically pumped cesium beam atomic clock," Opt. Express **28**, 6868 (2020).
31. T. Talvard, P. G. Westergaard, M. V. DePalatis, *et al.*, "Enhancement of the performance of a fiber-based frequency comb by referencing to an acetylene-stabilized fiber laser," Opt. Express **25**, 2259 (2017).
32. B. Wang, X. Peng, H. Wang, *et al.*, "Laser-frequency stabilization with differential single-beam saturated absorption spectroscopy of ^{4}He atoms," Rev. Sci. Instrum. **93**, 043001 (2022).
33. D. Hou, J. Wu, S. Zhang, *et al.*, "A stable frequency comb directly referenced to rubidium electromagnetically induced transparency and two-photon transitions," Appl. Phys. Lett. **104**, 111104 (2014).
34. S. Wu, C. Wang, C. Fourcade-Dutin, *et al.*, "Direct fiber comb stabilization to a gas-filled hollow-core photonic crystal fiber," Opt. Express **22**, 23704 (2014).
35. H.-B. Wang, H.-N. Han, Z.-Y. Zhang, *et al.*, "An Yb-fiber frequency comb phase-locked to microwave standard and optical reference," Chin. Phys. B **29**, 030601 (2020).
36. E. B. Kim, "Optical frequency comb comparison between optical clock mode and optical frequency synthesizer mode," Opt. Eng. **50**, 023602 (2011).
37. A. A. Filonov, S. A. Kuznetsov, V. S. Pivtsov, *et al.*, "The effect of ambient temperature fluctuations on the output frequency instability of the fiber femtosecond frequency comb," Laser Phys. Lett. **20**, 095101 (2023).
38. B. J. Chun, Y.-J. Kim, and S.-W. Kim, "Inter-comb synchronization by mode-to-mode locking," Laser Phys. Lett. **13**, 085301 (2016).
39. Y. Li, X. Hu, H. Cheng, *et al.*, "All-fiber acetylene-referenced optical frequency comb," Opt. Commun. **531**, 129233 (2023).
40. D. Ai, T. Jin, T. Zhang, *et al.*, "Absolute frequency measurement of the 6s6p $^3P_0 \rightarrow 5d6s\ ^3D_1$ transition based on ultracold ytterbium atoms," Phys. Rev. A **107**, 063107 (2023).
41. P. G. Westergaard, J. W. Thomsen, M. R. Henriksen, *et al.*, "Compact, CO_2-stabilized tuneable laser at 2.05 microns," Opt. Express **24**, 4872 (2016).
42. P. G. Westergaard, "Laser spectroscopy in hollow-core fibers: principles and applications," in *Applications of Molecular Spectroscopy to Current Research in the Chemical and Biological Sciences* (InTech, 2016), p. 365.
43. C. Wang, N. V. Wheeler, C. Fourcade-Dutin, *et al.*, "Acetylene frequency references in gas-filled hollow optical fiber and photonic microcells," Appl. Opt. **52**, 5430 (2013).
44. J. Hald, J. C. Petersen, and J. Henningsen, "Saturated optical absorption by slow molecules in hollow-core photonic band-gap fibers," Phys. Rev. Lett. **98**, 213902 (2007).
45. M. Triches, M. Michieletto, J. Hald, *et al.*, "Optical frequency standard using acetylene-filled hollow-core photonic crystal fibers," Opt. Express **23**, 11227 (2015).
46. P. Balling, M. Fischer, P. Kubina, *et al.*, "Absolute frequency measurement of wavelength standard at 1542 nm: acetylene stabilized DFB laser," Opt. Express **13**, 9196 (2005).
47. M. Kusaba and J. Henningsen, "The $\nu_1+\nu_3$ and the $\nu_1+\nu_2+\nu_4^1+\nu_5^{-1}$ combination bands of $^{13}C_2H_2$: linestrengths, broadening parameters, and pressure shifts," J. Mol. Spectrosc. **209**, 216 (2001).
48. K. Knabe, S. Wu, J. Lim, *et al.*, "10 kHz accuracy of an optical frequency reference based on $^{12}C_2H_2$-filled large-core kagome photonic crystal fibers," Opt. Express **17**, 16017 (2009).
49. Y. Zhu, Z. Cui, X. Sun, *et al.*, "Fiber-based dynamically tunable Lyot filter for dual-wavelength and tunable single-wavelength mode-locking of fiber lasers," Opt. Express **28**, 27250 (2020).
50. Y. Zhang, S. Fan, L. Yan, *et al.*, "Robust optical-frequency-comb based on the hybrid mode-locked Er:fiber femtosecond laser," Opt. Express **25**, 21719 (2017).
51. Z. Deng, Y. Liu, Z. Zhu, *et al.*, "Ultra-precise optical phase-locking approach for ultralow noise frequency comb generation," Opt. Laser Technol. **138**, 106906 (2021).
52. D. Ma, Y. Cai, C. Zhou, *et al.*, "37.4 fs pulse generation in an Er:fiber laser at a 225 MHz repetition rate," Opt. Lett. **35**, 2858 (2010).
53. P. Zhang, B. Rao, M. Li, *et al.*, "Long-term frequency-stabilized Er:fiber-based optical frequency comb with nonlinear amplifying loop mirror," Proc. SPIE **12169**, 121695U (2022).